Liquid Crystals
Publication details, including instructions for authors and subscription information:
http://www.informaworld.com/smpp/title~content=t713926090

Structural and electro-optical investigations of the smectic phase of chlorine-substituted banana-shaped compounds

G. Pelzl

Online publication date: 06 August 2010

To cite this Article Pelzl, G.(1999) 'Structural and electro-optical investigations of the smectic phase of chlorine-substituted banana-shaped compounds', Liquid Crystals, 26: 3, 401 — 413
To link to this Article: DOI: 10.1080/026782999205182
URL: http://dx.doi.org/10.1080/026782999205182

LIQUID CRYSTALS, 1999, VOL. 26, NO. 3, 401–413

Structural and electro-optical investigations of the smectic phase of chlorine-substituted banana-shaped compounds

G. PELZL*, S. DIELE, S. GRANDE†, A. JÁKLI‡, CH. LISCHKA, H. KRESSE, H. SCHMALFUSS, I. WIRTH and W. WEISSFLOG

Institut für Physikalische Chemie, Martin Luther-Universität Halle-Wittenberg, Mühlpforte 1, D-06108 Halle/S., Germany

†Fakultät für Physik and Geowissenschaften, Universität Leipzig, Linnéstraße 5, D-04103 Leipzig, Germany

‡Central Research Institute for Solid State Physics, P.O. Box 49, H-51525, Budapest, Hungary

(*Received 27 July 1998; accepted 12 October 1998*)

Six members of a new homologous series of achiral banana-shaped molecules have been synthesized and studied by optical microscopy, differential scanning calorimetry, NMR spectroscopy and X-ray diffraction. According to X-ray diffraction measurements on oriented samples, four homologues form an X_{B2} phase which exhibits antiferroelectric switching behaviour. From electro-optical studies the spontaneous polarization and the tilt angle could be measured. An orientational order parameter of 0.8 was determined by ^{13}C NMR and this is nearly independent of the temperature. NMR investigations also give information about the real conformation of the molecules in the X_{B2} phase. Dielectric measurements indicate that the rotation around the molecular long axis is clearly hindered because of the packing of the bent molecules within the smectic layers.

1. Introduction

More than 20 years ago Meyer *et al.* [1] discovered ferroelectricity in tilted smectic phases of chiral compounds. Later on, antiferroelectric smectic phases were also found in chiral materials [2]. As predicted by theoretical investigations, ferroelectricity or antiferroelectricity should not be restricted to chiral liquid crystals provided that asymmetric non-centrosymmetric molecules can build up a polar arrangement. Prost and Barois [3], as well as Petschek and Wiefling [4] predicted a ferroelectric smectic A phase where the spontaneous polarization is directed along the normal to the smectic layers. In a tilted ferroelectric smectic phase of a non-chiral compound, the vector of spontaneous polarization must be in the tilt plane [4, 5] or in the layer plane as shown by Brand *et al.* [6]. The first evidence of ferroelectricity in a non-chiral tilted smectic phase was found by Tournilhac *et al.* [7] in polyphilic compounds. Later Soto Bustamente *et al.* [8] reported the antiferroelectric behaviour of a mixture of an achiral side chain polymer with its monomer. In both cases, a spontaneous polarization could be determined by pyroelectric measurements, but no electro-optical response was observed. In 1996, Niori *et al.* [9] detected ferroelectricity in a smectic phase formed by banana-shaped achiral molecules. From X-ray measurements they concluded that the angled molecules are uniformly arranged in the bend direction. Such a structure possesses a C_{2v} symmetry, while the direction of the spontaneous polarization should be in the direction of the two-fold symmetry axis [6]. Ferroelectric switching was found in the smectic high temperature phase, but in contrast to the SmC* phase, the optical picture of the switched states was found to be independent of the polarity of the electric field [10]. In contrast to refs. [9, 10], Heppke *et al.* [11] and Weissflog *et al.* [12, 13] concluded in favour of an antiferroelectric switching behaviour from the current response. This was confirmed by Link *et al.* [14] who proposed a new structural model which explained the results of the electro-optical measurements.

In this paper we present new banana-shaped molecules which possess a chlorine in the 4-position on the central ring. Structural investigations on the smectic mesophase were performed by X-ray diffraction and NMR measurements. The electro-optical behaviour and the dielectric properties will be discussed on the basis of the structure of this phase.

*Author for correspondence.

Journal of Liquid Crystals ISSN 0267-8292 print/ISSN 1366-5855 online
http://www.tandf.co.uk/JNLS/lct.htm
http://www.taylorandfrancis.com/JNLS/lct.htm

2. Materials

Table 1 shows the general formula of three series of banana-shaped molecules which are distinguished by the substituents R and R'. In this paper we focus on 6 members of series II where chlorine is substituted in the 4-position (carbon 10 in the NMR studies). For comparison, series I and III are given because some data are used for the interpretation of NMR and dielectric measurements on members of series II.

The phase nomenclature follows the preliminary recommendation agreed at the International Workshop 'Banana-Shaped Liquid Crystals: Chirality by Achiral Molecules', Berlin (December 1997). New phase names are used because the mesophases of banana-shaped compounds are in no case completely miscible with smectic phases formed by calamitic mesogens. We use here symbol X_B instead of B to stress the preliminary character of these symbols until the complete structural characterization of the phases and to exclude confusion with respect to the SmB phase.

Compound **2** exhibits the mesophase X_{B1} which is also found in the short chain members of series I [10, 15]. The texture of the mesophase observed for compounds **3**–**6** reminds one of the texture of the switchable mesophase X_{B2} of series I studied by several groups [10–12]. The mesophases of the homologous compounds **3**–**6** are completely miscible with each other indicating the same phase type.

As shown in figure 1 the clearing points increase with increasing length of the terminal alkyloxy chains, and the melting points decrease. Therefore, the existence range of the X_{B2} phase becomes broader for the longer chain derivatives. This is of advantage for further measurements.

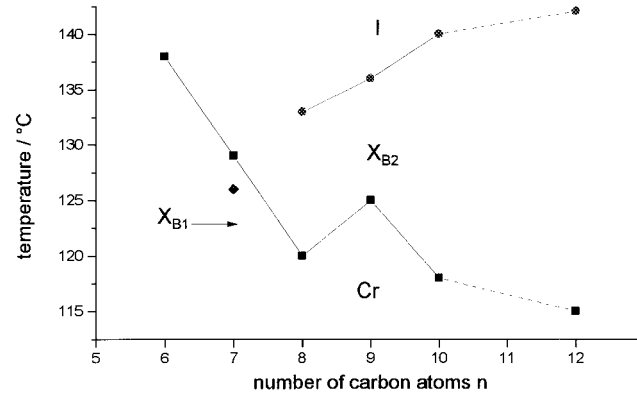

Figure 1. Transition temperatures of the compounds **1**–**6** as a function of the length of the terminal alkyloxy chains.

Table 1. Transition behaviour of the 4-chloro-1,3-phenylene bis-[4-(4-*n*-alkyloxy-phenyliminomethyl)benzoates **1**–**6**.

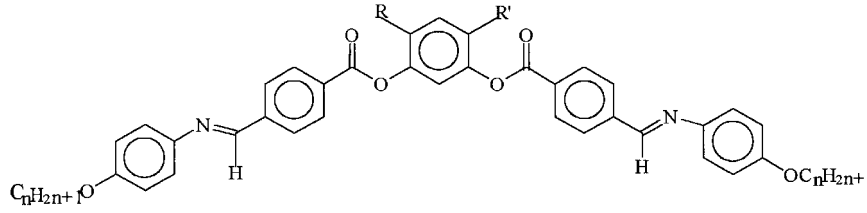

Series I: R = H; R' = H [9–12]
Series II: R = H; R' = Cl no. **1**–**6**
Series III: R = Cl; R' = Cl [18]

Compound No.	n	Cr	Temperature/°C [Enthalpy/kJ mol^{-1}]	X_{B1} [a]		X_{B2} [a]		I
1	6	•	138 [38.7]	—		—		•
2	7	•	130 [60.8]	•	(124) [17.8]	—		•
3	8	•	120 [33.2]	—		•	133 [16.8]	•
4	9	•	125 [15.5]	—		•	136 [14.8]	•
5	10	•	118 [—]	—		•	140 [—]	•
6	12	•	115 [16.8]	—		•	142 [16.5]	•

[a] After the 17th International Liquid Crystal Conference in Strasbourg (July 1998) the German and Japanese groups now prefer the code letters B_1, and B_2 instead of X_{B1} and X_{B2}, respectively.

It should be noted that Akutagawa *et al.* [16] synthesized isomeric chloro-substituted compounds which are only distinguished from series II by the direction of the azomethine group, but the phase behaviour is completely different. All members of that series exhibit a monotropic or enantiotropic nematic phase, and for some homologues an additional monotropic SmC phase is reported.

2.1. *Synthesis of the new materials*

The 4-chloro-1,3-phenylene bis[4-(4-alkyloxyphenyliminomethyl)benzoates] **1**–**6** were synthesized by esterification of 4-chlororesorcinol with the appropriate 4-(4-*n*-alkyloxyphenyliminomethyl)benzoic acid according to the method of Steglich [17] using dicyclohexylcarbodiimide. The preparation of the substituted benzoic acids that are themselves liquid crystalline up to high temperatures will be described elsewhere [18]. The purification of the final products is not simple and was performed by flash chromotography on aluminium oxide and by repeated recrystallization.

4-Chlororesorcinol (2.0 mmol) and the appropriate 4-*n*-alkyloxyphenyliminomethylbenzoic acid (4.0 mmol) were dissolved in absolute dichloromethane (100 ml) and dicyclohexylcarbodiimide (5 mmol) and 4-dimethylaminopyridine were added as catalyst. The mixture was stirred at room temperature for about 48 h. The dicyclohexylurea formed was filtered off and the solvent evaporated. The product was recrystallized twice from ethanol/dimethylformamide. Then the substance dissolved in chloroform was purified by chromatography on neutral aluminium oxide. Finally, the product was recrystallized repeatedly from toluene/heptane. Yields: 23–35%.

The analytical data are given for the heptyloxy derivative, compound **2**: ^{1}H NMR (200 MHz, $CDCl_3$) δ (ppm): 8.595 (s, 1H, CH=N), 8.59 (s, 1H, CH=N), 8.33 (d, 2H, Ar-H, $J = 8.4$ Hz), 8.28 (d, 2H, Ar-H, $J = 8.4$ Hz), 8.05 (d, 2H, Ar-H, $J = 8.4$ Hz), 8.04 (d, 2H, Ar-H, $J = 8.4$ Hz), 7.59 (s, 1H, Ar-H), 7.55 (s, 1H, Ar-H), 7.27 (m, 5H, Ar-H), 6.95 (d, 4H, Ar-H, $J = 8.8$ Hz), 4.00 (t, 4H, OCH_2, $J = 6.4$ Hz), 1.81 (m, 4H, OCH_2CH_2), 1.25 (m, 16H, CH_2), 0.91 (m, 6H, CH_3). Elemental analysis: $C_{48}H_{51}N_2O_6Cl$ (M_m: 787.40: calc. C, 73.22; H, 6.53; N, 3.56; found C, 73.40; H, 6.43; N, 3.55%.

3. Experimental

The thermal behaviour was investigated using a Perkin Elmer DSC7 differential scanning calorimeter. The texture and the field-induced change of the texture were examined using a polarizing microscope (Leitz Orthoplan) equipped with a Linkam hot stage (THM 600/S). X-ray experiments on non-oriented samples were performed with a focusing Guinier goniometer (Huber Diffraktionstechnik GmbH). Oriented samples were obtained by long annealing of a drop of the liquid crystal placed on a glass plate. In this case the X-ray beam was incident parallel to the glass plate. The X-ray patterns were obtained using a 2D detector (HI-Star, Siemens AG). Because of the special sample preparation, only the scattered intensity of the upper half of the reciprocal space could be recorded.

The NMR measurements were made with a Bruker MSL 500 spectrometer at a field of 11.7 T. The samples were put in standard 5 mm tubes. The proton decoupled ^{13}C spectra at 125 MHz, without spinning, are well resolved in the isotropic phase. Simple pulse excitations and cross-polarization experiments with mixing times between 1 ms and 5 ms were used. Proton decoupling in the liquid crystalline phase was performed by HP irradiation or WALTZ-cycles. The amplitude of the decoupling field was as low as possible (0.6–0.8 mT) to avoid heating of the sample. The efficiency of the HP decoupling depends markedly on the proton frequency off-set (0.5–3 kHz against the methylene resonance) and helps to identify the lines.

Dielectric measurements were performed using a double plate capacitor ($A = 2\,cm^2$, $d = 0.02$ cm) using the HP 4192 A and the Solartron Schlumberger SI 1260 impedance analysers. All attempts to orient the sample by an external magnetic field of maximum 0.7 T failed.

The electro-optical measurements were carried out using commercially available polyimide coated ITO test cells (EHC). We used a normal experimental set-up where the cell is heated on the hot stage of a polarizing microscope and a power supply (8116 A, Hewlett-Packard) generates the voltage signals. The field-induced change of light transmission was measured by a photomultiplier placed on the microscopic tube. The change of light transmission was monitored by a 500 MHz oscilloscope (54503 A, Hewlett-Packard) and then transferred to a computer terminal for further analysis.

Spontaneous polarization was measured with the triangular wave voltage method using the same experimental set-up.

4. Experimental results

4.1. *X-ray investigations*

The X-ray pattern of a non-oriented sample of the smectic phase of compound **3** is shown in figure 2. In the small angle region, equally spaced Bragg reflections (3 orders) are observed indicating the smectic layer structure. From the diffraction angle θ, the thickness d of the smectic layers of 3.66 nm was determined at 123°C. The d-values slightly increase with decreasing temperature (3.70 nm at 60°C). On the other hand, the diffuse scattering in the wide angle region ($\theta \sim 10°$) gives evidence that there is no long range positional order within the layers.

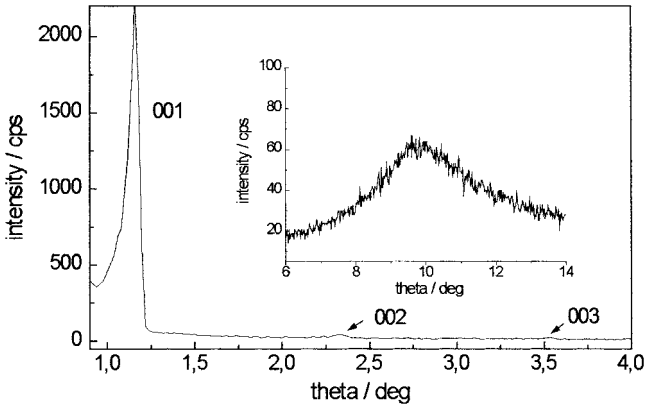

Figure 2. X-ray diffraction pattern of the X_{B2} phase of compound **3** (123°C).

The pattern of a well oriented monodomain is presented in figure 3. It is seen that the layer reflections are on the meridian of the pattern, whereas the diffuse scattering maxima in the wide angle region are located out of the equator. The angle between these two diffuse scattering maxima measured by a χ-scan was found to be 105°, corresponding to a tilt angle of about 37°. The pattern of the oriented sample clearly points to the X_{B2} phase which was already reported in refs. [12, 13].

For compound **6** we also obtained well oriented samples. From the X-ray pattern we could determine a d-value of 4.24 nm and a tilt angle of about 33°.

The heptyloxy homologue (compound **2**) forms another smectic phase which exhibits a mosaic texture and which cannot be switched on applying an electric field. The X-ray pattern of a non-oriented sample shows a diffuse scattering in the wide angle region indicating the absence of in-plane order within the smectic layers. But in the small angle region, three sharp Bragg reflections are observed, the d-values of which are $d_1 = 3.11$ nm; $d_2 = 2.14$ nm and $d_3 = 1.36$ nm. Up to now we have not obtained oriented samples of this phase, and therefore a structural model cannot be proposed. On the other hand, the X-ray pattern is quite similar to that found for the lower homologues of the unsubstituted compounds of series I which is designated as X_{B1} [15] or SmA_b [19]. Recently X-ray measurements on oriented samples of these substances could be performed and indicate a two dimensional smectic phase with a rectangular unit cell

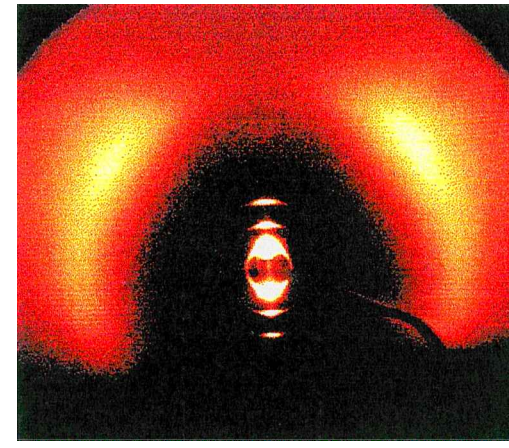

(*a*)

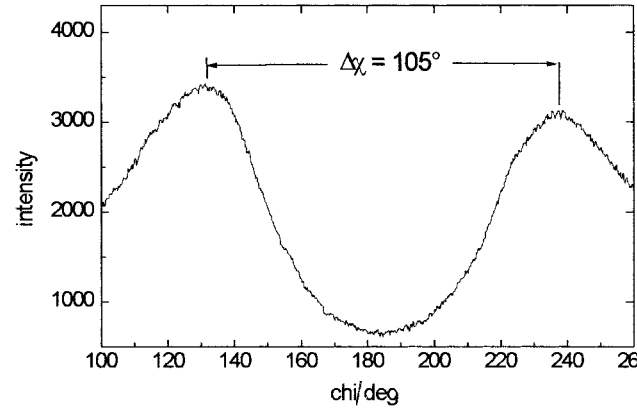

(*b*)

Figure 3. (*a*) X-ray pattern of an X_{B2} monodomain of compound **3** (128°C); (*b*) χ-scan.

[19]. Using the same indexing (1 0 1; 0 0 2 and 1 0 3, respectively) the data for compound **2** can also be described by a rectangular cell with the lattice parameters $a = 4.52$ nm and $c = 4.28$ nm.

4.2. *NMR investigations*

NMR investigations were carried out on compound **3** which exhibits an X_{B2} phase. The numbering of the carbon positions is given in the following formula:

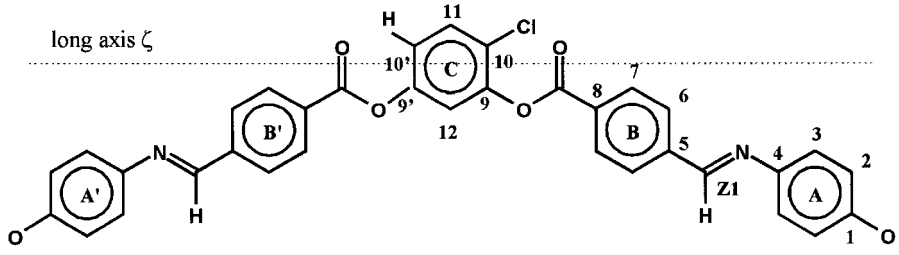

The local surroundings for the rings A on the right and left side are identical, providing equal isotropic shifts. The different substituents at C10 and C10′ disturb the mirror symmetry of ring C so removing even the equivalence of the rings B visible in a small difference of the isotropic shifts for C7, C8 and COO. Most carbons are resolved, but there is no clear signal assignable to C11 due to overlapping with C7 and C8. The assignment of the lines in the isotropic spectrum shown in figure 4(*a*) rests upon the increment system and comparison with the unsubstituted and dichloro banana-shaped molecules of series I and III. Because of non-linear substituent effects, the assignment of C9 and C9′ can also be exchanged. All measurements were carried out with decreasing temperature. The transition to the liquid crystalline phase occurs for this substance within a few degrees. The director aligns parallel to the external field. The spectrum in the smectic phase of compound **3** shown in figure 4(*b*) offers a large number of lines that overlap strongly in some regions. The line shifts increase smoothly with decreasing temperature within the smectic phase. An important support in the assignment of the lines is a small dependence of their intensity or line width on the experimental NMR parameters (the relaxation time is longer and CP enhancement is weaker for non-protonated C, the optimal decoupling efficiency for low power irradiation ranging between 3000 and 2000 Hz of proton off-set for different carbon positions in the rings). Further assistance comes from the comparison with the simpler spectra of banana-shaped molecules of series I and III [13, 18]. Applying these results, we propose the assignment shown in figure 4(*b*), but especially for the peaks of just one quaternary carbon in the molecule, uncertainty remains. The *ortho*-carbons of ring A and B (C2, C3, C6, C7) illustrate apparently different anisotropic shifts of equivalent positions in the two halves. The difference in the conformation decreases along the aromatic substituents. The *para*-carbons (C1, C4, C5, C8)

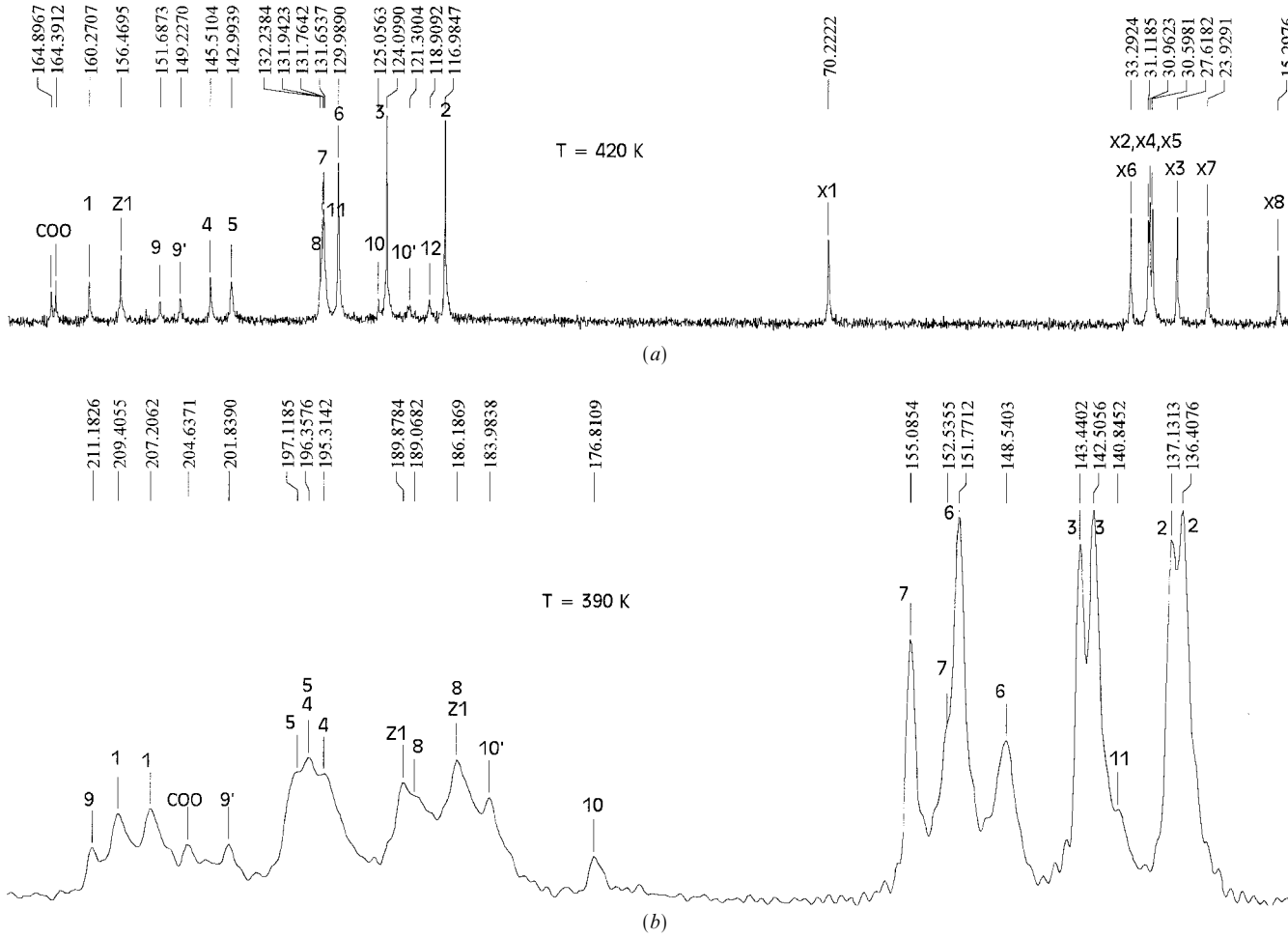

Figure 4. (*a*) Isotropic ^{13}C spectrum of compound **3** at 420 K obtained with single pulse excitation and igated WALTZ-decoupling. (*b*) The spectrum in the smectic phase at 385 K is obtained by cross-polarization with a mixing time of 3 ms and 10 ms HP decoupling with a proton off-set of 3 kHz.

as assigned in the spectrum support this fact. We expect a smaller peak for C4 due to the C–N dipole interaction. The same was true for banana-shaped molecules of Series I and III. Using this finding, the line shape at 196 ppm can be well fitted. The high power necessary for the decoupling of the peak at 183 ppm enables us to identify it with C10. The increase in the intensity with growing mixing time is typical for quaternary carbons. In connection with the anisotropic shifts of the C9, C10 and C9′ in banana-shaped molecules of series I and III [13, 18], the C9, C10 and C9′ were assigned as shown in figure 4(*b*). There remains some uncertainty concerning the assignment of the COOs. The small line is broadened and there is no clear signal assignable to the second ester group due to overlapping. All available information was used to find the correct assignments.

For a quantitative interpretation, a relation between the shift tensor, the orientational ordering and the conformation is needed. For the moment the main interest concerns the conformation of the molecule. We use a simple model of separate averaging and neglect contributions from biaxial order fluctuations (*D*). This yields the equation [20]:

$$\delta^i_{\mathrm{obs}}(T) = \delta^i_{\mathrm{iso}} + S\delta^i_{\zeta\zeta} \qquad (1)$$

where $\delta^i_{\zeta\zeta}$ is the component of the shift tensor in the molecular frame ξ, η, ζ with ζ as the molecular long axis, and S the orientational order parameter. This tensor component contains all information about the conformation. The equation gives the order parameter in the chosen local frame. The chosen molecular frame should nearly coincide with the main frame of the ordering matrix. However, contrary to the symmetric substituted banana-shaped molecules, a symmetry plane does not exist. Nevertheless we assume a long axis lying symmetric in the plane of ring C as shown in the formula and prove the correctness of this choice by the experimental results.

The four observed lines from ring C enable us to calculate the order parameter S and the direction of the long axis, provided that the main axis tensor components are well known. In fact we only know the components in the molecular frame of disubstituted banana-shaped molecules [13, 18] (table 2). Using these values an approximate calculation of the main frame tensor values can be done ($\delta^9_{11} = 90$ ppm, $\delta^9_{22} = 9$ ppm, $\delta^{10}_{11} = 100$ ppm, $\delta^{10}_{22} = 9$ ppm for banana-shaped compounds of series I, and $\delta^9_{11} = 93$ ppm, $\delta^9_{22} = 9$ ppm, $\delta^{10}_{11} = 83.3$ ppm, $\delta^9_{22} = 15$ ppm for those of series III). The isotropic shifts of C10′ in compound **3** agree with the values of the corresponding positions in the disubstituted molecules and we expect the same main axis components, too. The isotropic shifts for C9′s are different from the disubstituted banana-shaped molecules. A change in the isotropic shifts is connected with new tensor components, but there are no rules for the variation of the tensor components with substitution on ring C. We expect values similar to and between the components mentioned above. The uncertainty in our knowledge of the tensor components is too large to apply equation (1).

Starting from the opposite point of view, an order parameter $S = 0.8$ can be assumed similar to that for other banana-shaped molecules ($S = 0.81$ for the unsubstituted compound [13]). Then the molecular frame components are obtained as given in table 2. The two extracted $\delta^{10}_{\zeta\zeta}$ differ only by 2 ppm from values of the disubstituted molecules (table 2). Considering the uncertainty of S, the angle of the long axis with the bond directions C10–*R* deviates not more than 1 degree

Table 2. The tensor components $\delta^i_{\zeta\zeta}$ (ppm) for banana-shaped molecules and for a suitable linear reference molecule[a] with an equivalent ring A.

Samples	Series I	Series III	H, Cl-ban[c]	H, Cl-ban[d]	Ref[a]
C1	52.8	81.6	58.7	61.3	83.2
C2	21.7	35.3	24.7	25.4	34.8
C3	20.7	32.4	23.1	24.2	33.5
C4	55	83.8	62.4	64.1	84.9
C5	57.1	92	65.5	68.3	89.2
C6	20.8	36.7	23.7	27.7	40.8
C7	22.7	39	26.2	29.4	36.1
C8	59.5	89.6	67.9	70.9	84.5
C9	70.8	72	64.9	74	
C10	77.2	66.2	77.4	64.2	
COO	43.6	27.2	49		61.5[b]
CHN	32.6	53.9	37.5	41.3	51.5

[a] Reference substance: $C_7H_{15}O–C_6H_4–CH=N–C_6H_4–OC_8H_{17}$.
[b] Value obtained from $CH_3O–C_6H_4–COO–C_6H_4–OC_6H_{13}$.
[c] H, Cl-ban corresponds to the unsubstituted side half of the molecule;
[d] H, Cl-ban corresponds to the chloro-substituted half of the molecule.

from 30° in the direction of C10′. The deviation of $\delta^9_{\zeta\zeta}$ from the values of the symmetric molecules originates mainly from a change in the tensor components, and geometrical conclusions are not realistic. An alignment of the long axis which is symmetric but out of the plane of ring C reduces all $\delta^i_{\zeta\zeta}$ by nearly the same amount (5 ppm for an angle of 10°). We cannot exclude this geometry with $S = 0.85$ and respectively, lower $\delta^i_{\zeta\zeta}$ and an out of plane angle of 10°, but for further calculations we prefer the lower value $S = 0.8$ with the direction of the long axis as shown in table 1. The order parameter S increases by 0.01 with decreasing temperature over the smectic phase range of 15 K.

Now we apply the order parameter to the shifts of the carbons in the branches. We include the small temperature dependence and extract the $\delta^i_{\zeta\zeta}(T)$ for the C^i belonging to the substituted rings and linkage groups. The results are given in table 2. Included in this table are also values for the corresponding symmetric substituted materials and a suitable two ring reference molecule [($C_7H_{15}O$–C_6H_4–CH=N–C_6H_4–OC_8H_{17}: Cr 61 (SmA 58.5) N 87 I]. The second aromatic ring of the reference molecule has the same substituents as ring A in the banana-shaped molecules. Since the isotropic shifts agree exactly, their tensor components in the main axes system should also be the same.

As seen from table 2 the tensor components of the C^i in the chosen molecular system have values between those of the symmetric banana-shaped compounds of series I and III. The conformation of the two molecular halves is different for the left (H, Cl) and right side (H, Cl) and deviates from the conformations of symmetric bananas.

The relation between the long axis shift tensor component and the main frame values is given by

$$\delta_{\zeta\zeta} = \delta_{11}\cos^2\beta + \left[-\frac{\delta_{11}}{2} + \left(\frac{\delta_{11}}{2} + \delta_{22}\right)\cos(2\varphi)\right]\sin^2\beta. \quad (2)$$

Here β describes the tilt angle between long axis and *para*-axis of the rings and φ the torsion of the ring plane starting with the long axis within the plane (see figure 5). The application of equation (2) requires knowledge of the main frame components δ_{11} and δ_{22} for each position of the ring. These values are not exactly known. We made measurements for the reference molecule in the liquid crystalline phase and obtained the tensor components in the molecular frame also cited in table 2. Furthermore, we assume that the molecular long axis lies nearly parallel to the *para*-axes which is characteristic for linear two ring compounds. Now we interpret these values as δ_{11} and assume standard values for the δ_{22}. The main frame components are then optimised for the smallest deviations in β and φ calculated from different positions of one ring for all banana-shaped compounds.

The application of equation (2) leads to the angles given in figure 5. The absolute values depend smoothly on the assumed S. A reduction of S to 0.75 decreases

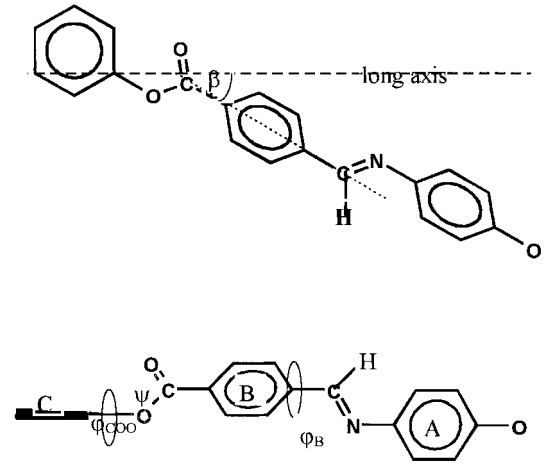

Figure 5. Conformation of the half-parts for monochloro-substituted molecules derived from the value of ^{13}C tensor components of the rings A and B. The torsion of the ring planes in the picture is arbitrary and does not agree with the estimated values presented in the inserted table.

	β_B	φ_B	β_A	φ_A	φ^{COO}	ψ^{COO}	φCHN
H,Cl-b	24.5	51.6	24.2	46.7			91
H,Cl-b	24.3	45.2	25.4	46.9	66	5	96

The angles β, φ and ψ are given in degrees.

the angle β by 2.5° and leaves the φ nearly constant, but the differences between the two halves do not change. The tilt angles β for the other two cited molecules were obtained with the same main frame tensor components as 29° and 7° for banana-shaped compounds of series I and III, respectively [13, 18].

The calculated conformational data are averaged values in the sense of the NMR time scale of 10^{-5} s. Due to the symmetry, there is no possibility for NMR to distinguish between a plus and a minus torsion and therefore also a fast exchange between the two conformations may exist.

It is surprising that the angles for the monosubstituted molecules are so different from those of the symmetric materials. The first explanation is a deviation of the molecular long axis from the symmetric position by nearly 10° in the direction of the C–Cl bond with nearly the same conformation of the corresponding half-parts as in the disubstituted banana-shaped compounds. This contradicts the observed shifts of C10′ and C10 which exclude a deviation of the long axis by more than 1° from the 30° symmetric direction as already discussed. So this model fails to explain the observations. Then a molecular system with a long axis out of the plane of ring C remains. This occurs only if in the time average the left and right branches are aligned in opposite directions of the plane of ring C. This needs chiral-like interactions, but we have not enough information to postulate such a conformation. Besides, with a tilt of the branches and of the long axis, the angle between both axes remains nearly unchanged and does not explain the experimental results. So it seems more realistic that the conformations of the two branches really deviate from the geometry found in the disubstituted banana-shaped compounds. It follows that not only the intramolecular interactions with nearest neighbours, but also those with more distant substituents are important for the conformation of mobile segments.

The conformation of the half-parts is mainly given by the geometry of the COO linkage at ring C. Unfortunately we could assign only one COO to a line and this with a higher uncertainty. The obtained tensor component is larger than for the symmetric banana-shaped compounds (table 2). A simple torsion of the COO-plane around the bond from ring C to the oxygen (φ^{COO}) would only slightly change the angles of the *para*-axes of rings B and A. There must be a second rotation around the O–C(O) bond of the ester group (ψ^{COO}) (figure 5) to explain tilt angles lower than 25°. For larger angles, the outer bonds of the ester group no longer lie on a plane. One obvious explanation for the measured $\delta_{\zeta\zeta}^{COO}$ is $\varphi^{COO} = 65°$ and $\psi^{COO} = 5°$, but in fact we have only one measured value and two unknown angles. The different conformation of the two linkage groups is still an open question. In the dichloro-substituted banana-shaped molecules, the plane of the ester group aligns nearly perpendicular to the plane of ring C (figure 5) with a torsion ψ^{COO} of *c.* 30° around the second bond. One source of the molecular dipole moment of the banana-shaped molecules is the ester groups. A torsion of the ester plane reduces the component along the bow in the molecule, but for the derived torsion of 65°, a component still remains as experimentally observed. For the dichloro-compound with a torsion of nearly 90°, the component of the dipole moment is zero [18].

The anisotropic shifts of the carbons belonging to the chains are small (2 to 5 ppm) and only resolved for proton off-set lower than 1000 Hz. Most peaks are resolved in the smectic phase, but no splitting is observed for the carbons in the two branches. The $\delta_{\zeta\zeta}^{Cxn}$ are similar to values found in unsubstituted banana-shaped compounds (series I) with a relatively low value for $x1$ (in comparison to linear molecules) and larger shifts in the central part of the chain. However, all components in the molecular frame up to the sixth position are by 1–2 ppm smaller than the values of equivalent chain carbons in linear reference compounds. The last segments have similar shifts to linear molecules that indicate a more extended form of the chains in the outer regions. Because of the smallness of the shifts the error is large. All components increase smoothly with decreasing temperature. The smaller value of all shifts beginning with the $-OCH_2-$ contradicts the model of a higher flexibility of the chains in these molecules.

4.3. *Dielectric measurements*

Dielectric investigations can give information about the dynamics of polar groups, of molecules as a whole or of collective processes [21, 22].

Experimental data for the dielectric loss ε'' versus frequency f and temperature υ for compound **3** are presented in figure 6. The strong increase of ε'' at low frequencies arises mainly from the conductivity. This will be discussed later. The dielectric absorption at higher frequencies could be observed in the isotropic and the X_{B2} phase, too. For the formal description, a Cole–Cole mechanism [23] and a term which considers the conductivity is used:

$$\varepsilon^* = \varepsilon_1 + \frac{\varepsilon_0 - \varepsilon_1}{(1 + i\omega\tau_1)^{1-\alpha_1}} + \frac{A}{f^n}. \qquad (3)$$

As an example, experimental data and the fitted curve are given in figure 7. In this way the static dielectric constants ε_0, the high frequency limits ε_∞, the relaxation times τ_1 and the Cole–Cole distribution parameters α at different temperatures were calculated. In figure 8 the relaxation times in the isotropic and X_{B2} phases of compound **3** are plotted versus the reciprocal absolute

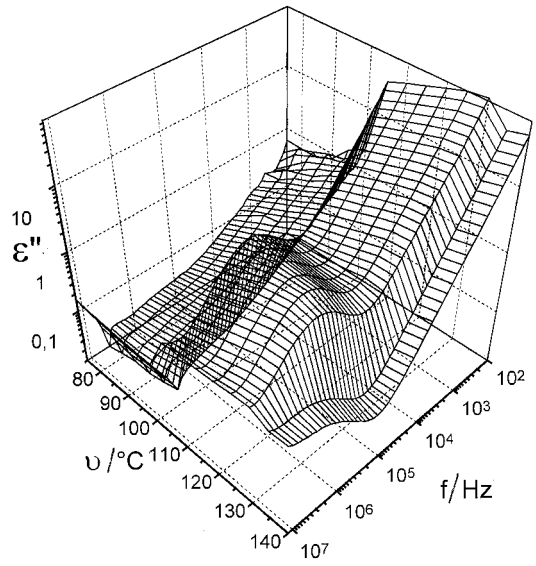

Figure 6. 3D plot of the dielectric loss ε'' versus frequency and temperature for compound **3**.

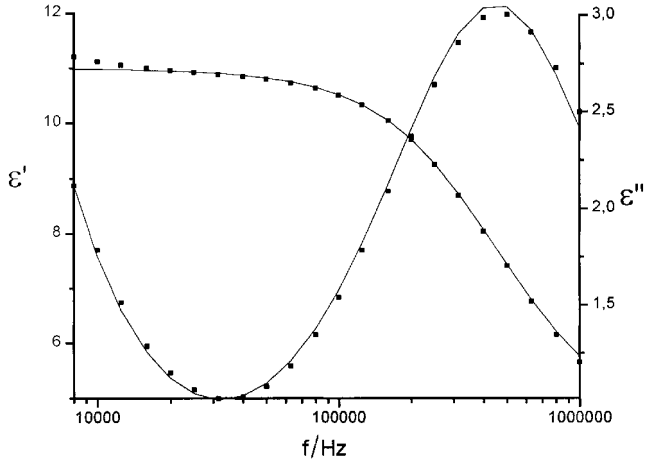

Figure 7. Dielectric dispersion and absorption curves for compound **3** at 129°C. $\varepsilon_0 = 11.01$; $\varepsilon_1 = 4.39$; $\tau_1 = 0.354\ \mu s$; $A = 1.59 \times 10^4\ s^{-1}$, $n = 1.0$.

temperature. Additionally τ_1-values for the nematic and SmC̃ phases of an analogous compound of Series III [phase behaviour: Cr (97 SmC̃) 111 N 140 I] which contains two Cl-atoms in the middle part and a decyloxy-group at each end [18], are given. These molecules possess a symmetric structure which cannot give a dielectric response to the reorientation around the molecular short axis. Therefore, the detected absorption must be connected with reorientation around the molecular long axis which is shifted to lower frequencies due to the high viscosity of the sample [22].

The same molecular origin can be assumed for the motion in the X_{B2} phase of compound **3**. The small contribution from the reorientation around the molecular short axis should be observed at a thousand times higher

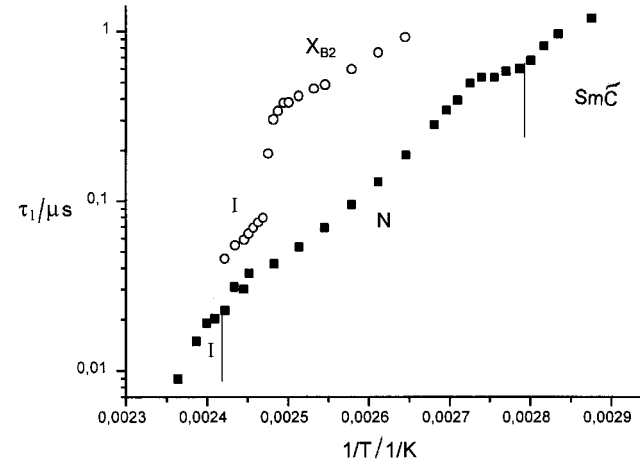

Figure 8. Relaxation times τ_1 for compound **3** (circles) and the reference substance (dichloro compound of series III) (squares) as functions of the reciprocal absolute temperature. The activation energies are $(50 \pm 2)\,kJ\,mol^{-1}$ for the X_{B2} phase and $(95 \pm 5)\,kJ\,mol^{-1}$ for the isotropic phase of compound **3**.

relaxation times. It is covered by the conductivity however. The clearly different behaviour of the relaxation times at the transition into the isotropic phase is important. Compound **3** shows a stepwise decrease of τ_1 by a factor of about 4. This means that the τ_1 reorientation around the molecular long axis is hindered by an additional potential in the X_{B2} phase. Assuming a potential with two minima at 0° and π during the rotation of the molecule around the angle 2π, one can expect the same and also different depths of the minima. In order to differentiate between these possibilities, static dielectric constants and ε_1-values are given in figure 9. It can be seen that ε_0 decreases with decreasing temperature.

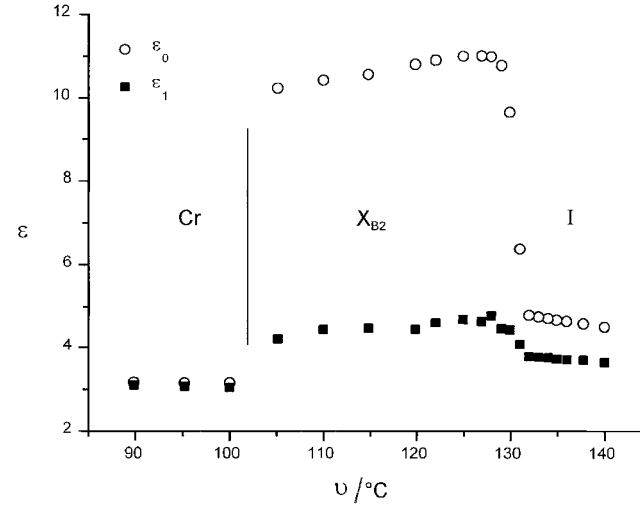

Figure 9. Static (ε_0) and quasi-static (ε_1) dielectric constants of compound **3** at different temperatures.

If one excludes changes in the orientation, this effect must be the result of an asymmetric potential. This means, in other words, that the banana-like molecules are preferably packed in the bent direction. Such an order should produce ferroelectricity if it is extended over macroscopic domains. In order to look for a collective reorientation of the domains, dielectric measurements were extended to 10 mHz. As demonstrated in figure 10, no clear relaxation effect could be seen. As in the publication of Sekine and coworkers [10] (who have probably not correctly interpreted their measured data) only the formation of an electrical double layer is detected. A careful analysis of the experimental data in a broader frequency range, as in figure 7, needs to consider an additional Cole–Cole mechanism with a low frequency absorption range, as shown in figure 11. This could not be detected in the isotropic phase. The dielectric increment of 7.5 for this mechanism is too high for the reorientation of the small longitudinal dipole moment, especially if one considers that the molecular long axes are oriented mainly perpendicular to the electrical measuring field (see figure 9, increase of ε_0 at the transition into the X_{B2} phase). It is possible that this absorption range is caused by a collective motion in the antiferroelectric clusters. In order to clarify the situation further, experiments on samples with a much lower conductivity are necessary. For this reason ferroelectricity or antiferroelectricity can be proven only by measurements of the polarization reversal current.

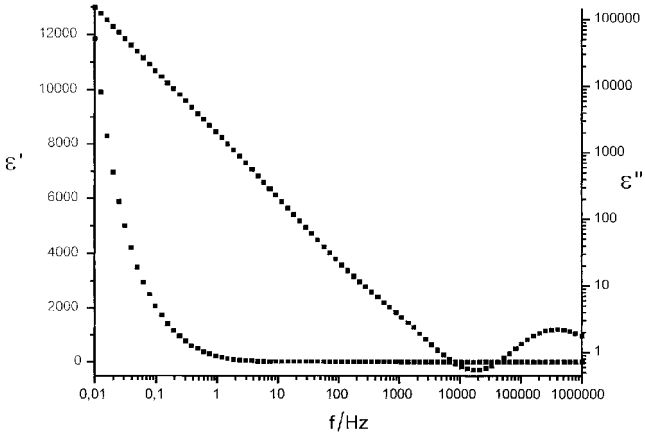

Figure 10. Dielectric absorption and dispersion curves at $\upsilon = 121°C$ for compound **3**.

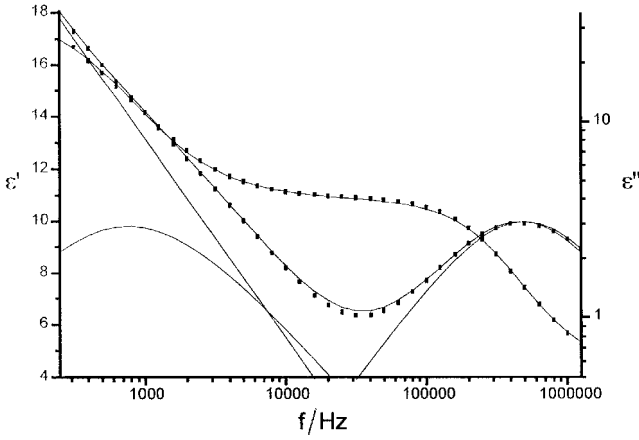

Figure 11. Fit parameters for compound **3** at $\upsilon = 129°C$; $\varepsilon_a = 18.3$; $\varepsilon_0 = 10.8$; $\varepsilon_1 = 4.34$; $\tau\alpha = 0.19$ ms; $\tau_1 = 0.335\ \mu$s; $\alpha_a = 0.172$; $\alpha_1 = 0.040$; $A = 8.96 \times 10^3\ s^{-1}$; $n = 1.0$.

4.4. *Electro-optical behaviour*

The switching processes observed by polarizing microscopy are rather complicated. On very slow cooling from the isotropic liquid, the X_{B2} phase appears as a grainy fan-shaped texture. Applying an electric field not higher than $1.5\ V\,cm^{-1}$, the switched states are independent of the polarity of the field. If the applied voltage increases, stripes parallel to the smectic layers occur. The threshold for the formation of the stripes decreases with increasing temperature. With increasing voltage, the number of stripes increases, but above a saturation value the stripes nearly disappear. If the voltage is switched off, the stripes reappear and partially remain also in the off-state. If the voltage is switched off very fast, the formation of the stripes is suppressed and the X_{B2} phase appears as a smooth fan-shaped texture which reminds one of the SmA fan-shaped texture. This texture, which can be also obtaind by a high a.c. voltage, was the subject of electro-optical investigations.

Figure 12 shows the electric response of a 4 μm thick cell under a triangular wave voltage for compound **6**. The frequency of the field was 100 Hz, the amplitude ±42.5 V. It is seen that two current peaks were recorded during a half period, indicating an antiferroelectric behaviour which was also found for the X_{B2} phases of

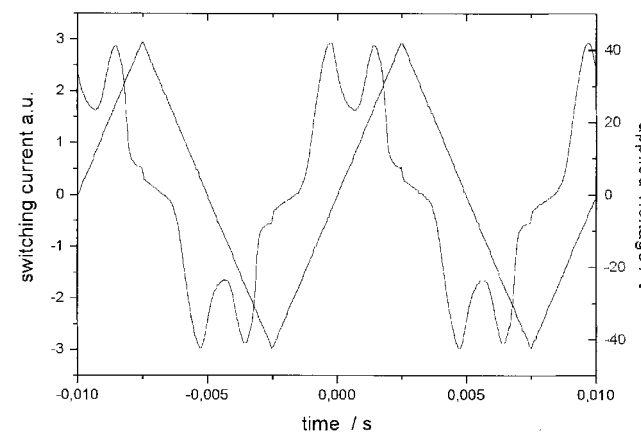

Figure 12. Switching current response in the X_{B2} phase of compound **6** obtained by applying a triangular voltage (±42.5 V; 100 Hz).

other compounds [11–14]. The spontaneous polarization determined by integration of the switching current peaks was found to be 640 nC cm^{-2} at 10 K below the clearing point (see figure 13).

Figure 14 shows the fan-shaped texture of the X_{B2} phase in a 10 μm thick cell without field and on applying an electric field. It is seen that the texture is different for an inverse sign of the applied electric field. Dark regions of figure 14 (*a*) correspond to bright ones of figure 14 (*c*). This difference indicates a polar order and is particularly clear when domains with circular bending of the layers occur. In these domains the smectic layers are more or less parallel to the substrates and form circles around the centre of the domains. This is indicated by a black extinction cross which coincides with the directions of the crossed polarizers. On the other hand, this means that the optical axes are parallel or perpendicular to these directions. When an electric field is applied, the orthogonal extinction brushes rotate clockwise or anticlockwise depending on the sign of the applied field (see figure 15). The maximum rotation angle at a saturation voltage (~40 V) was found to be about 40° at 128°C and 34° at 131°C. It should be noted that in oval domains, the rotation of the extinction cross could also be observed.

The field-induced rotation of the extinction cross was first described and analysed in the excellent paper of Link *et al.* [14]. This effect can only be explained if we assume that the planes of the banana-shaped molecules are not only arranged in the bend direction [9], but, in addition, are tilted with respect to the smectic layer planes [14]. The tilt of the molecules on the one hand and the polar order of the bent molecules on the other hand are two independent symmetry-breaking factors which cause a chirality of the smectic layers where the handedness depends on the tilt direction of the molecules.

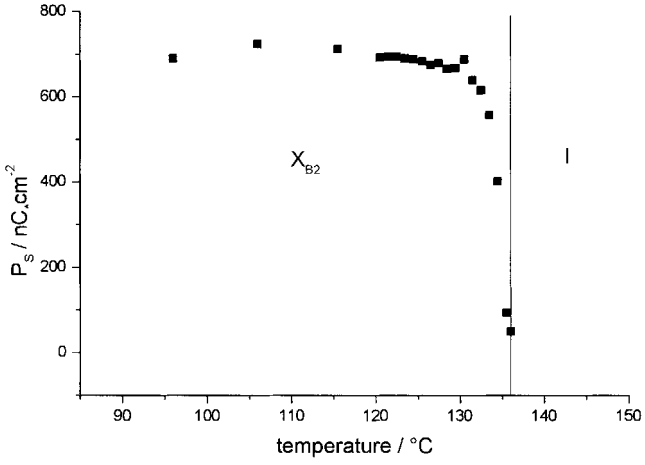

Figure 13. The spontaneous polarization $\mathbf{P}_S$ of the X_{B2} phase of compound **6** as a function of temperature.

This means that, for a given tilt angle, two equivalent layers with antiparallel polar axes can exist which are mirror images of each other. According to [14] there are two equilibrium structures which should be antiferroelectric. In the 'racemic' state (*R*-state) the layer polar direction alternates in sign from layer to layer, but the layer tilt is uniform, meaning that the handedness alternates. On applying a sufficiently high electric field, optically equivalent ferroelectric states arise independently of the sign of the field. If the flower-like domain with circular bending of the smectic layers occurs in the *R*-state, the extinction cross should rotate in only one direction, independently of the polarity of the field. In the homogeneous chiral state (*H*-state) the tilt direction and the polarity alternate from layer to layer, but the handedness is uniform. In this case the extinction brushes rotate in opposite directions dependent on the polarity of the field. Provided that the smectic layers are arranged perpendicular to the substrates (book-shelf geometry) the average optical axes of the switched states are distinguished by twice the tilt angle. Under our experimental conditions the homogeneous chiral (*H*) state is obviously predominant. In a first approximation, the measured maximum rotation angle can be identified with the tilt angle of the molecules within the smectic layers (40° ... 30°).

In the model of Link *et al.* [14], the formation of fringes can be interpreted as domains with oppositely tilted directors. This is in contrast to Sekine *et al.* [25] who suggest that the fringes indicate a spontaneous formation of the helix.

The orientation of the grainy texture into a smooth fan-shaped texture can be interpreted as reorientation of the polar axes on application of an electric field. As shown by Jákli *et al.* [26], in the original grainy texture, the smectic layers are bent or tilted with respect to the substrate planes so that the direction of the spontaneous polarization is not parallel to the electric field. For this reason a vertical field acts as a mechanical torque on the smectic layers which causes an orientation of the smectic layers more or less perpendicular to the substrates.

5. Conclusions

As shown in §4.2, the conformation of the banana-shaped molecules in the smectic X_{B2} phase of compound **3** could be analysed by NMR spectroscopy. Although this analysis is much more difficult than for the analogous unsubstituted compounds of series I the NMR measurements give clear evidence that the molecules are angled, where the bending angle between the two half-parts ($\gamma = 180°\text{-}2\beta = 131°$) is higher than that found for compounds of series I (120°, see [13]). On the other hand, for analogous dichloro-substituted compounds (series III), the molecules are nearly stretched in the

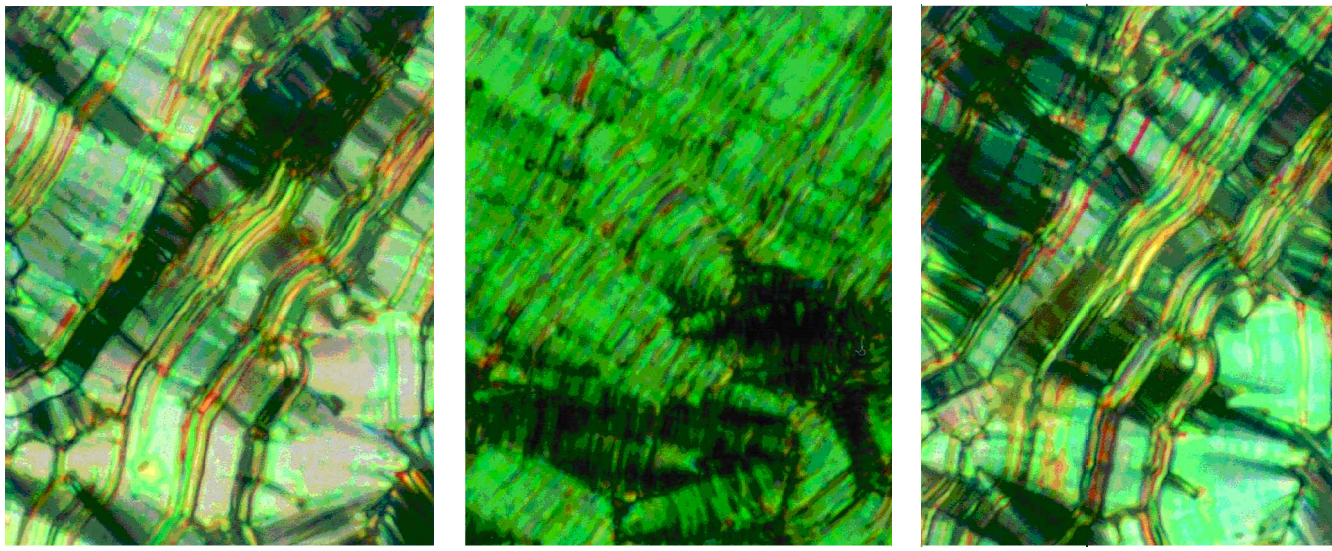

(*a*) (*b*) (*c*)

Figure 14. X_{B2} fan-shaped texture of the X_{B2} phase of compound **3**: (*a*) + 30 V, (*b*) 0 V and (*c*) − 30 V. Sample thickness 10 μm, temperature 125°C.

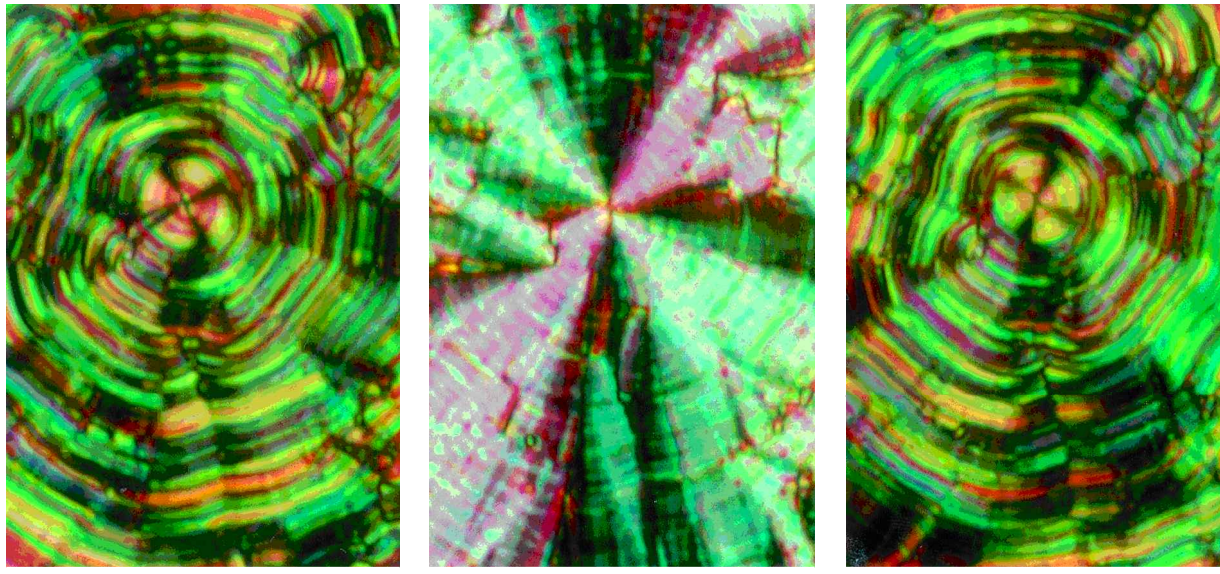

(*a*) (*b*) (*c*)

Figure 15. Rotation of the extinction cross of the X_{B2} phase of compound **3**: on applying an electric field (*a*) + 20 V, (*b*) 0 V, (*c*) − 20 V. Sample thickness 10 μm, temperature 125°C.

liquid crystalline and solid states ($\gamma \sim 165°$ [18]), so that these compounds can be regarded as calamitic compounds which form nematic or normal smectic phases (SmC, SmC̆). This comparative consideration indicates that a critical bending angle (at least 131°) is necessary for the formation of typical X_B phases. It follows from electro-optical investigations (§4.4) that the planes of the banana-shaped molecules are tilted by about 40° with respect to the layer normal of the smectic X_{B2} phase. Also from X-ray investigations on oriented samples, a tilt angle could be determined ($\sim 37°$) which can be due to the tilt of the whole molecule or the tilt of the halves of the molecules with respect to the layer normal. We cannot distinguish between these different influences, but our results show that this value is mainly determined by the tilt of the whole molecules, because an orthogonal alignment of the bent molecules within the smectic layers would cause a tilt of the mesogenic units of about 25°.

The orientational order parameter in the X_{B2} phase is relatively high (0.8) and does not change with temperature. This is a clear difference from analogous smectic phases without in-plane order for calamitic compounds.

There is also a clear difference in the dynamic behaviour. In the case of calamitic compounds, the relaxation time τ_1 related to the rotation of the molecules around the long axes is changed continuously at the transition from isotropic to SmA or SmC. In contrast, there is a stepwise decrease of τ_1 at the transition isotropic $\rightarrow X_{B2}$, indicating an additional rotational hindrance as a result of an asymmetric potential.

All the experimental facts lead to the conclusion that compounds with banana-shaped molecular structure represent a new sub-field of thermotropic liquid crystals which have no counterpart in the class of calamitic liquid crystals.

References

[1] Meyer, R. B., Liebert, L., Strelecki, I., and Keller, P., 1975, *J. Phys. Fr. Lett.*, **36,** L69.

[2] Chandani, A. D. L., Ouchi, Y., Takezoe, H., Fukuda, A., Terashima, K., Furukawa, K., and Kishi, A., 1989, *Jpn. J. Appl. Phys.*, **28,** L1261.

[3] Prost, J., and Barois, P., 1983, *J. chim. Phys.*, **80,** 65.

[4] Petschek, R. G., and Wiefling, K. M., 1987, *Phys. Rev. Lett.*, **59,** 343.

[5] Tournilhac, F., Bosio, L., Nicoud, J.-F., and Simon, J., 1988, *Chem. Phys. Lett.*, **145,** 452.

[6] Brand, H. R., Cladis, P., and Pleiner, H., 1992, *Macromolecules*, **25,** 7223.

[7] Tournilhac, F., Blinov, L. M., Simon, J., and Yablonski, S. V., 1992, *Nature*, **359,** 621.

[8] Soto Bustamente, E. A., Yablonski, S. V., Ostrovski, R. J., Beresnev, L. A., Blinov, L. M., and Haase, W., 1996, *Liq. Cryst.*, **21,** 829.

[9] Niori, T., Sekine, F., Watanabe, J., Furukawa, T., and Takezoe, H., 1996, *J. mater. Chem.*, **6,** 1231.

[10] Sekine, T., Takanashi, Y., Niori, T., Watanabe, J., and Takezoe, H., 1997, *Jpn. J. appl. Phys.*, **36,** L-1201.

[11] Heppke, G., Jakli, A., Krüerke, D., Löhning, C., Lötzsch, D., Paus, S., Rauch, S., and Sharma, N. K., 1997, Abstracts, European Conference on Liquid Crystals, Zakopane, Poland.

[12] Weissflog, W., Lischka, Ch., Benné, I., Scharf, T., Pelzl, G., Diele, S., and Kruth, H., 1997, *SPIE*, **3319,** 14.

[13] Diele, S., Grande, S., Kruth, H., Lischka, Ch., Pelzl, G., Weissflog, W., and Wirth, I., 1998, *Ferroelectrics*, **212,** 169.

[14] Link, D. R., Natale, G., Shao, R., Maclennan, J. E., Clark, N. A., Körblova, E., and Walba, D. M., 1997, *Science*, **278,** 1924.

[15] Heppke, G., private communication.

[16] Akutagawa, T., Matsunaga, Y., and Yasuhara, K., 1994, *Liq. Cryst.*, **17,** 659.

[17] Neises, B., and Steglich, W., 1978, *Angew. Chem.*, **90,** 556.

[18] Weissflog, W., Lischka, Ch., Diele, S., Pelzl, G., Wirth, I., Grande, H., Kresse, H., Schmalfuss, H., Hartung, H., and Stettler, A., *Mol. Cryst. liq. Cryst.* (submitted).

[19] Watanabe, J., Niori, T., Sekine, T., and Takezoe, H., 1998, *Jpn. J. appl. Phys.*, **37,** L-139.

[20] Riede, A., Grande, S., Hohmuth, A., and Weissflog, W., 1997, *Liq. Cryst.*, **22,** 157.

[21] Kresse, H., 1983, *Advances in Liquid Crystals*, edited by G. H. Brown, Vol. 6, p. 109.

[22] Kremer, F., Vallerien, S. U., and Zentel, R., 1990, *Adv. Mater.*, **2,** 145.

[23] Hill, N. R., Vaughan, W. E., Price, A. H., and Davies, M., 1946, *Dielectric Properties and Molecular Behaviour* (van Nostrand, Reinhold).

[24] Kresse, H., Ernst, S., Wedler, W., Demus, D., and Kremer, S., 1990, *Ber. Bunsenges. Phys. Chem.*, **94,** 478.

[25] Sekine, T., Niori, T., Watanabe, J., Furukawa, T., Choi, S. W., and Takezoe, H., 1997, *J. mater. Chem.*, **7,** 1307.

[26] Heppke, G., and Moro, D., 1998, *Science*, **279,** 1872.

[27] Jakli, A., Lischka, Ch., Weissflog, W., Rauch, S., and Heppke, G., *Mol. Cryst. liq. Cryst.* (submitted).